Comparison of two microwave radiobrightness models and validation with field measurements

William L. Crosson, Charles A. Laymon, *Member, IEEE,* Ramarao Inguva, Christine Bowman

Abstract-- This paper compares microwave brightness temperature (T_B) estimated by two radiobrightness models--a multi-layer coherent radiative transfer (CRT) model and a single-layer Fresnel reflectance model. Two dielectric mixing schemes were used along with the models to calculate permittivity (real part of the dielectric constant). Model T_B and permittivity estimates were inter-compared and validated against Huntsville '98 field experiment measurements. Model differences can be attributed to the mixing scheme, the radiobrightness model, or the vertical profile representation. Two sets of simulations were performed to quantify the sources of variation, one using observed soil temperature and moisture profiles as input, and another using uniform profiles. Using uniform profiles, systematic differences in permittivity estimated by the mixing schemes resulted in T_B differences as large as 15 K. However, for uniform profiles, differences in T_B estimated by the radiobrightness models for a given permittivity value were less than 2 K. For cases using observed profiles, near-surface drying of the profiles resulted in T_B values from the CRT model 6-10 K higher than estimates from the Fresnel model, which determines T_B based on 0-5 cm mean moisture and temperature. Therefore, the major sources of T_B variations were the dielectric mixing scheme and the shape of the near-surface moisture profile. No radiobrightness/mixing scheme combination exhibited superiority across all plots and times.

Keywords: permittivity, microwave radiometry, soil measurements

---

This work was supported by Universities Space Research Association (USRA) NCC8-140 under NASA Grant NCCW-0084 with Alabama A&M University's Center for Hydrology, Soil Climatology and Remote Sensing (HSCaRS).
W. Crosson and C. Laymon are with Universities Space Research Association, Global Hydrology and Climate Center, 320 Sparkman Dr., Huntsville, AL 35805 (bill.crosson@msfc.nasa.gov).
R. Inguva is with East-West Enterprises, Huntsville, AL 35805.
C. Bowman is with the University of New Hampshire, Durham, NH 03824.
Corresponding Author: William L. Crosson Phone: 256-961-7913 Fax: 256-961-7788

I. Introduction

An emerging technology that is contributing to our ability to estimate vertical soil moisture profiles involves coupling microwave measurements from aircraft or satellite sensors with models of soil water dynamics. The accuracy of such models suffers from uncertainties in soil properties, meteorological input data and model physics. As a result, soil moisture estimates may diverge from reality, but intermittent observations of remotely-sensed soil moisture can be used to adjust modeled soil moisture, if only in the uppermost layers. Soil moisture remote sensing has reached a state of maturity after more than two decades of research, although some problems remain unsolved. Previous investigations have used remote sensing observations at various wavelengths, mainly from ground-based and aircraft sensors, to estimate surface soil moisture and have compared results with surface measurements or hydrological model-estimated soil moisture [1-4]. The success of these efforts has varied depending on space and time scales and sensor wavelength. As shown in [5], the complex nature and diurnal evolution of near-surface moisture gradients impart difficulties on remote sensing of soil moisture.

There has been a considerable amount of soil moisture research noting the advantages of passive microwave observations at L-band (~1.4 GHz) because of its deeper penetration depth and lower sensitivity to vegetation cover, and L-band sensors have shown some ability to estimate near-surface soil moisture [1, 2, 5-8]. For technological reasons, the only remote sensors planned for satellite missions in the next few years that may be useful for soil moisture estimation will operate at much higher C-band frequencies (6–7 GHz). These include the Advanced Microwave Scanning Radiometer (AMSR), to be launched in 2001 on the Aqua satellite and in 2002 on ADEOS-II. Currently, L-band microwave sensors are not in operational use, being deployed only from ground or aircraft platforms. However, there is a strong conviction within the land surface hydrology community that L-band remote sensing

holds the greatest promise for useful soil moisture retrieval, and an L-band sensor is an integral component of the Soil Moisture-Ocean Salinity mission, planned for a 2005 launch. Other L-band systems for future satellite deployment are under development.

Associated with the development of microwave sensors has been an emphasis on soil moisture retrieval algorithms. Microwave remote sensing techniques employ a wide range of soil moisture retrieval methods, from inverse radiative transfer models based on multi-frequency microwave brightness temperature (T_B) to much simpler models using single-frequency data to estimate surface soil moisture. In inverse radiative transfer models, soil moisture and temperature profiles are estimated using *a priori* information from the soil model to constrain the inverse solution [9-11]. Before an inverse method is applied, the ability of the associated forward model to accurately estimate T_B, and the model's sensitivity to inherent uncertainties in input variables and parameters, need to be evaluated. Forward radiobrightness models can be separated into two classes–multi-layer radiative transfer models and single-layer models. The term radiobrightness model is used here in reference to any model that estimates microwave brightness temperature or emissivity from principally soil moisture and temperature. In the process of determining emissivity, a dielectric mixing model is first applied to determine soil dielectric properties. Single-layer models treat the soil medium as a single homogeneous slab characterized by 'effective' temperature and moisture values.

Radiative transfer models may be further classified as coherent or non-coherent. A coherent model considers the phase associated with reflections between soil layers of varying dielectric constant whereas a non-coherent model does not. In the latter, the emitted microwave radiation from each model layer is calculated directly from the radiative transfer equation, and the amount of energy transferred between layers is determined by the reflectivity calculated from the Fresnel equations [12].

A few previous studies have focused on validation of radiobrightness models with microwave brightness temperature measurements or comparison of results produced by such models. In [13], brightness temperatures estimated by the coherent radiative transfer (CRT) model used in our study were compared to analytical solutions of the radiative transfer equation based on a set of synthetic moisture and temperature profiles. The agreement at L-band was within approximately 5 K, with model temperatures being slightly lower than analytical values. Field soil moisture profile measurements were used to validate the same CRT in [14]; modeled brightness temperatures slightly underestimated observed values for dry soil and slightly overestimated observed temperatures for wet soil. These small disparities were attributed to imperfect representation of the near-surface moisture profiles. The CRT model produces more accurate results than simpler models in cases of complex moisture profiles, but by the same token is more sensitive to errors in the moisture profile [13, 14]. A comparison of coherent and non-coherent models conducted by [12] indicated that the models agreed to within about 4 K at L-band. The largest differences between models occurred when the near-surface moisture gradient was greatest.

The objective of this paper is to utilize soil moisture and temperature profile measurements made at very high vertical resolution as the basis for comparing L-band brightness temperature and dielectric constants estimated by two radiobrightness models in conjunction with two dielectric mixing models. The two radiobrightness models are diverse in terms of detail of the soil medium, with one being a multi-layer coherent radiative transfer model, whereas the other is a simple Fresnel reflectance-based model that treats the emitting layer as uniform.

II. Data

A. Experimental setting - Huntsville '98

The Huntsville '98 field experiment (Hsv98) was conducted near Huntsville, Alabama from 15-28 June 1998 with the objective of simultaneously measuring soil moisture using passive and active microwave sensors and *in situ* instruments. The research testbed is located at Alabama A&M University's Winfred Thomas Agricultural Experiment Station 20 km north of Huntsville. The testbed, which is nearly level, consisted of six 30 x 50 m plots--one without vegetation, one with a fescue cover, and four with corn. The corn was planted with a row spacing of 50 cm. It was approximately 110 cm tall at the beginning of the experiment and grew to about 190 cm by the conclusion. One day before the experiment, individual corn plants were harvested at ground level from three of the four corn plots to produce plots with plant densities of one-third (Corn-1), one-half (Corn-2), and two-thirds (Corn-3) of full density (Corn-4). Surface soil texture of the testbed is clay loam to silt loam. The total organic matter content in the upper 15 cm is less than 2%.

At the beginning of the field experiment the upper soil layer was quite dry. Measured volumetric water content (VWC) for the upper 10 cm layer at the beginning of the experiment ranged from 16-24% across the plots. The deeper soil, however, was much wetter, with VWC in the range of 24-40% below 15 cm. In order to sample much wetter conditions, irrigation was applied to all plots on 15 June. The amount of water applied to the plots averaged 20-30 mm, but due to windy conditions, application was very non-uniform. Rainfall occurred on four occasions during the experiment: June 16th (1.4 mm), 19th (12.5 mm), 20th (2.4 mm), and 25th (20.3 mm). Due to rainfall interception by the canopy, some of the rainfall did not reach the ground, especially for lower rain amounts on the Corn-4 plot. In fact, for the experimental period only 15.6 mm of rain (in addition to irrigation) was recorded at the soil surface in the Corn-4 plot, although this amount does not include the flow of water down the corn stalks. By comparison, 37.4 mm was recorded on the Bare plot and 26.7 mm at Corn-2. Excellent drying

conditions existed between the rain events. The driest conditions occurred just before the 25 June rainfall when near-surface moisture content on all plots was slightly lower than at the beginning of the experiment.

B. S and L band Microwave Radiometer (SLMR)

The S (2.65 GHz) and L (1.413 GHz) band Microwave Radiometer (SLMR) is a dual-frequency passive sensor system [7]. The radiometers were mounted to observe horizontal polarization. An Everest 4000A thermal infrared sensor with 7.5-15 μm bandpass obtained spot measurements of surface temperature. In normal operation, radiometer data were acquired at a look angle of 15° from nadir and at a nominal height of 14 m. Measurements were made at least several times on each plot during the day throughout the experiment. This study is limited to SLMR measurements at L-band, the most promising wavelength for eventual satellite applications. Another reason for restricting the analysis to L-band is the significant vegetation density in the field experiment which led to very little sensitivity to soil moisture at the S-band wavelength.

The radiometers were calibrated using a two-point calibration equation based on external hot and cold reference targets. The hot load measurements were acquired by placing microwave absorbing panels at ambient temperature (~300 K) over the radiometer antennae. The sky at 160° from nadir served as the cold load reference (~5 K). These references exceed the range of normal observations. Both reference targets were measured frequently throughout the day. A time-series of the T_B observed for each reference target showed that the sensor response was stable. Measurements were made previously over water (~110 K) to verify the linearity of the response in each instrument. Measurement errors are estimated to be less than ±2 K.

The theory behind microwave remote sensing of soil moisture is based on the large contrast between the dielectric properties of liquid water (~ 80) and dry soil (< 4) which has been studied by several investigators (e.g., [15-17]). For typical soil moisture applications using low altitude sensors at longer microwave wavelengths, energy emitted by the atmosphere and sky can be neglected, so that the T_B of the land surface is related to the thermometric soil surface temperature, T_{sfc}, through emissivity such that

$$T_B = eT_{sfc} = (1\text{-}R)T_{sfc} \quad (1)$$

where R is surface reflectivity and e = (1-R) is effective emissivity, dependent on the dielectric constant of the medium [8]. T_B can be corrected for surface roughness [18] and vegetation effects [19] and used to determine emissivity for a smooth soil surface, which is related to the dielectric constant for non-nadir incidence as described by the Fresnel reflectivity [20]. Although the relationship between emissivity and T_B is very nearly linear, the relationship between emissivity and dielectric constant is nonlinear.

C. Near-surface (0-5 cm) soil profile (NSP) data from gravimetric measurements

Soil samples for gravimetric soil moisture determination were collected with a coring device immediately outside of the SLMR footprint. A 5.4 cm diameter core barrel was lined with a 6.0 cm stack of 0.5 and 1.0 cm brass rings. The corer was hammered into the soil and extracted. The brass rings and enclosed soil were then removed intact from the barrel. The soil core was sliced between the rings to produce discrete soil layers, which were weighed before and after oven drying to determine gravimetric soil moisture for the following layers: 0.0-0.5, 0.5-1.5, 1.5-2.5, 2.5-3.5, 3.5-4.5 and 4.5–5.0 cm. On one occasion, the dry bulk density of each layer was determined to allow conversion of gravimetric soil moisture measurements to volumetric water content.

D. Soil profile measurements

1) Volumetric Water Content

During Hsv98, soil moisture and temperature sensors were deployed at four soil profile sites located approximately 10 m from the SLMR footprint. Volumetric water content was measured at ten depths (3, 5, 7, 10, 15, 20, 30, 40, 50 and 60 cm) on each plot with CS615-L Water Content Reflectometers (WCR) manufactured by Campbell Scientific, Inc. (CSI). This device uses time-domain reflectometry to measure VWC. Horizontal placement in the soil confined the WCR sampling volume to about 4 cm in the vertical direction. Soil-specific calibration of the WCRs was performed which includes a correction for temperature effects. The result of the calibration was a quadratic regression equation between WCR measurements and observed VWC (determined from gravimetric water content using bulk density derived for each core) applicable to the soil at each profile site. The temperature correction improves the accuracy of the sensors, particularly by removing an apparent diurnal soil moisture fluctuation that results from temperature variations. Error analysis based on the calibration data indicate the accuracy of the WCRs to be better than ±1.5% VWC when temperature compensation is applied, or better than ±3% VWC without temperature compensation. Absolute errors are smaller at low soil moisture levels.

A comparison of VWC measured by the WCRs at 3 cm depth (representative of the 1-5 cm layer) with the mean 0-5 cm VWC derived from the near-surface profile measurements (not shown) indicated excellent agreement for the Bare plot, but large differences for the Corn-2 and Corn-4 plots. The mean WCR soil moisture estimates for Corn-2 are much higher than the mean 0-5 cm VWC from coincident NSP observations (28% vs. 19% VWC). For Corn-4, the mean difference is even greater (33% vs. 16% VWC). These differences, which are quite consistent throughout the experiment, are not completely understood. They may be due to spatial variability caused by non-uniform irrigation or to the influence of roots. Because the NSP observations provide the model input, whereas the 3 cm WCR measurements

are used only to validate output of the models, we have adjusted the WCR VWC measurements for their apparent wet bias to the mean of the NSP 0-5 cm VWC measurements. This was done for each plot by adding to the WCR 3 cm measurements the difference between the mean of all available NSP observations and the mean of the coincident WCR measurements. The VWC adjustments were 0.5% for the Bare plot, -8.9% for Corn-2 and -16.6% for Corn-4.

2) *Soil Temperature*

At each site, soil temperature measurements were made using CSI 107B sensors at five profile depths (3, 7, 15, 30 and 50 cm). In addition, a 0-5 cm (nominally 2.5 cm) mean soil temperature was measured using CSI model TCAV averaging thermocouple probes installed at 1, 2, 3 and 4 cm. Soil surface temperatures for the Bare plot were measured by the thermal infrared sensor incorporated with the remote sensing system.

3) *Permittivity*

Estimates of electrical permittivity, the real part of the dielectric constant, were derived from the Water Content Reflectometers. Such estimates are possible because of the relationship between permittivity and wave propagation time (Jim Bilskie, CSI, personal communication). In order to obtain the wave propagation time, we first determined the time delay of the sensor's internal electronics. The WCR oscillation period is equal to the time taken for the wave to travel up and down the probe two times, plus a delay due to internal circuitry:

$$t_{tot} = t_{prop} + t_{cir} = 4 \bullet t_{rod} + t_{cir} \quad (2)$$

where: t_{tot} = oscillation period

t_{prop} = total wave propagation time = $4 \bullet t_{rod}$

t_{rod} = time to traverse rod one-way

t_{cir} = time delay due to internal circuitry

The propagation velocity in a medium with electrical permittivity ε is given by:

$$V = c/(\varepsilon^{0.5}) \tag{3}$$

where c is the speed of light in a vacuum. V also can be expressed in terms of the probe length L:

$$V = L/t_{rod} \ . \tag{4}$$

Combining (2) – (4),

$$\varepsilon = (c/V)^2 = [c(t_{tot} - t_{cir})/4L]^2 \ . \tag{5}$$

Solving for the circuit delay time t_{cir},

$$t_{cir} = t_{tot} - 4L \bullet \varepsilon^{0.5}/c \ . \tag{6}$$

By taking laboratory WCR readings (t_{tot}) in a medium having known permittivity (i.e. air for which ε = 1), we calculated t_{cir} from (6). We assumed that t_{cir} varied between sensors (Jim Bilskie, personal communication) and determined it for each WCR. Equation (5) was then used to calculate ε from *in situ* measurements in the soil, using individual sensor t_{cir} values.

We also estimated the expected errors in permittivity due to uncertainty in the oscillation period t_{tot}. The observed sensor-to-sensor variability in t_{tot} was about ± 0.45 nsec. To determine the impact of this uncertainty on estimates of ε, we determined the relative error in wave propagation velocity V. To do so, we calculated the error in the total wave propagation time t_{prop}. From (2) and (6),

$$t_{prop} = t_{tot} - t_{cir} = 4L \bullet \varepsilon^{0.5}/c \ . \tag{7}$$

Assuming that all of the variability in the measured period is due to variability in t_{prop} and not in the circuit delay time, the relative error in t_{prop} is defined as (error in t_{tot})/t_{prop}. From (4), $V = 4L/t_{prop}$, so the

percent error in V is approximately equal (for small errors) to the percent error in t_{prop}. From (5), the relative error in ε is the square of the relative error in V. Table I gives percent errors for ε for various permittivities, and ranges of estimated ε, associated with an error in t_{tot} of 0.45 nsec. These limits represent worst-case uncertainty in estimating ε. As seen in Table I, the percent error in ε decreases with ε, but the absolute error increases from approximately ± 0.5 units for very dry soil to about ± 1.0 unit for wet soil.

E. Estimation of model parameters

Parameters that must be specified in the models relate to the SLMR system configuration and soil and vegetation properties (Table II). Sand and clay percents and soil porosities were measured in the field and varied slightly between the plots. The amount of water bound to the soil particles increases with clay content and was specified accordingly [16, 21]. Surface roughness was determined for the Bare plot by photographing a board with a reference grid and calculating the variance of the height distribution of the surface. The deep soil (10 m) temperature was set to 291 K (18^o C), the mean annual air temperature for Huntsville.

Vegetation parameters used in the models include vegetation water content and the vegetation b-parameter [19]. Vegetation water content was measured at several times during Hsv98, and the values generally increased with time. Time-varying values were used for simulations at each plot. The value for the vegetation b-parameter was taken from [19] based on previous experiments in Corn crops.

III. Models

Two radiobrightness models were used in conjunction with two dielectric mixing models to estimate L-band microwave brightness temperatures. Although the two radiobrightness models are quite different, two basic steps are used in each to convert soil moisture and temperature inputs to brightness temperature. First, the dielectric constant of the soil-water-air medium is estimated using one of the two dielectric mixing schemes. In the case of the multi-layer radiative transfer model, the dielectric constant is calculated independently for each soil layer, while for the Fresnel reflectance model it is calculated from mean near-surface conditions, thus producing an 'effective' dielectric constant. Second, the brightness temperature is estimated from the calculated dielectric constant profile or the effective value. The two radiobrightness models differ primarily in this aspect.

A. Dielectric mixing schemes

Two dielectric mixing schemes were used to determine the dielectric constant of the soil-water-air medium as a function of water content. The first is the Dobson mixing scheme, a power-law model relating the real and imaginary parts of the dielectric constant to that of each soil component [16]. The value of the empirical exponent α was set to 0.65 based on [16]. The second dielectric mixing scheme used in this study is that of Wang and Schmugge [15]. This mixing scheme (WS) was used to estimate only the real part of the effective dielectric constant (ε_{eff}) of the emitting layer from volumetric soil moisture observations. Unique equations describe the relationship between dielectric constant and soil moisture at moisture contents less than and greater than a transition moisture value that is an empirical approximation of the wilting point moisture. These equations require estimates of soil porosity, dielectric constants for ice and rock (from [17]), and formulations for the frequency and temperature-dependent real part of the complex dielectric constant for free water [20].

Differences in the real part of the dielectric constant estimated by the two mixing schemes as a function of VWC are shown in Fig. 1. Values of ε were calculated for VWC ranging from 5 – 50% using the Bare plot soil parameters. The Dobson model with $\alpha = 0.65$ produces higher permittivities, especially at moderate moisture contents (15-25% VWC) where the difference is as large as 2.5 units. Below 10% and above 35% VWC, differences are less than about 1.5 units. Bare plot permittivity as a function of VWC derived from WCRs (from (5) and the Bare plot calibration equation) is also included in fig. 1. Between 5% and 35% VWC, differences between the WCR curve and the two mixing schemes are less than 2 units, equivalent to a difference of less than 4% VWC. Above about 40%, the WCR estimates substantially higher permittivities than do the two mixing schemes, but such moisture contents did not occur in any of the plots during Hsv98.

B. Coherent Radiative Transfer Model

The first of the two radiobrightness models is a coherent radiative transfer model developed for a stratified medium characterized by potentially complex moisture and temperature profiles [13]. The model is based on the vertical profiles of temperature and emissivity, the latter of which is strongly controlled by the soil moisture content. Required input variables to the CRT are surface temperature, vegetation water content, and profiles of soil moisture, temperature and porosity. The moisture and temperature profiles are obtained from Hsv98 measurements. Values of model parameters are given in Table II.

The brightness temperature at horizontal polarization, neglecting the effects of surface roughness and vegetation, is given by:

$$T_{Bo} = \frac{k}{\cos\theta} \int_0^\infty T(z)\varepsilon(z)\left|\psi(z)\right|^2 dz \qquad (8)$$

where k is the free space wave number (= $2\pi/\lambda$, where λ is wavelength), θ is the observation angle from nadir, T(z) is temperature at depth z, $\varepsilon(z)$ is the complex dielectric constant, and $\psi(z)$ is subject to:

$$\frac{d^2\psi(z)}{dz^2} + [\varepsilon(z)k^2 - (k\sin\theta)^2]\psi(z) = 0 \quad . \tag{9}$$

Although soil moisture does not appear explicitly in (8)-(9), it comes into effect through its strong influence on $\varepsilon(z)$. For uniform profiles of T and ε, the solution of (8)-(9) is equivalent to that of the Fresnel reflectance function. For non-uniform profiles, a direct solution of (8)-(9) is not feasible. Therefore, the problem is reformulated into one consisting of a stratified soil having layers that are thin enough to be assumed of uniform temperature and dielectric constant. In so doing, the integral in (8) is replaced by a summation that accurately estimates the integral provided the thickness of the layer is small compared to the wavelength [13]. In the current study, the summation is performed using 100 soil layers of 0.7 cm thickness, giving a total depth of integration of 70 cm.

Because the observed microwave emission depends on the amount of scattering that takes place at the soil surface, compensation is required for surface roughness. A simple statistical method for correcting for the effects of surface roughness was developed by Choudhury *et al*. [18], in which the soil surface height is assumed to have a Gaussian distribution. The measured standard deviation of surface height was approximately 0.3 cm for the bare plot. A surface roughness value of 0.1 cm for the corn plots was found to give the best agreement between SLMR-measured and modeled brightness temperature. Including the correction for surface roughness of the bare plot yields a 'rough surface' L-band T_B that is up to 5 K greater than the 'smooth surface' brightness temperature T_{Bo} for dry to moderately wet soil, and the correction is somewhat greater for very wet soil.

In the presence of vegetation, energy is attenuated requiring a compensating correction. After an extensive review of research on the effects of vegetation on microwave energy transmission, Jackson

and Schmugge [19] proposed a simple model in which the transmissivity of the vegetation layer is parameterized in terms of the vegetation water content. This algorithm is very conducive to remote sensing applications because proxies for vegetation water content can be obtained by other remote sensing methods [22-24]. We used a variable value for the vegetation water content based on measurements.

C. Fresnel Reflectance Model

The other radiobrightness model used in this study, denoted FR, is a single-layer model based on the Fresnel reflectivity equation, which defines the behavior of electromagnetic waves at a smooth dielectric boundary [15]. Application of the Fresnel equation requires assumptions that the dielectric and temperature properties of the soil are uniform throughout the emitting layer, that emissivity is related principally to the real part of the complex dielectric constant, and that the soil depth emitting the energy, which is wavelength-dependent, is known. There are several additional considerations that also should be incorporated in a data retrieval algorithm. A comprehensive review of many of these issues are provided by [7].

At L-band, the real part (permittivity) is much larger than the imaginary part of the dielectric constant [17]. Nonetheless, the use of only the real part in the Fresnel model is a potential source of discrepancy between FR and the CRT, the latter of which incorporates the complex dielectric constant. This issue was examined in [25] in which estimates obtained via an inverse Fresnel soil moisture retrieval algorithm were applied to the forward CRT. Uniform soil moisture and temperature profiles were used, therefore any differences between brightness temperature calculated by the CRT and values input to the inverse algorithm can be attributed to effects of the imaginary part of the dielectric constant.

These differences were found to be less than 1 K, which is smaller than the measurement errors associated with microwave remote sensors.

From (1), it is clear that observed microwave emission depends on both soil moisture and temperature. Because soil moisture and temperature are not independent, we must normalize the observed brightness temperature by the effective radiating temperature of the soil if we are to relate T_B to soil moisture. As described by [26], effective temperature, T_{eff}, is defined as

$$T_{eff} = T_d + C\left(T_{sfc} - T_d\right), \tag{10}$$

where T_d is the deep (e.g. 10-15 cm) soil temperature and C is an empirically-defined weighting function based on the relative contribution of individual layers to the microwave emission at the soil surface. Normalizing T_B with respect to T_{eff} helps to reduce the diurnal hysteresis in the T_B-soil moisture relationship. As in the CRT model, the effects of surface roughness were accounted for using the technique of Choudhury *et al*. [18], and brightness temperature was adjusted for the effects of the plant canopy with the vegetation correction algorithm of Jackson and Schmugge [19].

IV. Experimental Design

A. Simulations with measured profiles

A number of simulations were performed using measured temperature and moisture profiles in order to inter-compare results from the CRT and FR models and validate the results using measured brightness temperatures and dielectric constants. Observations from three sites – Bare, Corn-2 and Corn-4 – supplied inputs to the two models. These sites were chosen to illustrate a range of vegetation conditions,

from no vegetation to the densest vegetation canopy at Corn-4. Three radiobrightness/mixing model combinations were utilized. The CRT model was run using both the Dobson ('CRT/Dobson') and Wang-Schmugge mixing schemes ('CRT/WS'), to examine differences in brightness temperature due solely to the mixing scheme. The CRT simulations utilized high-resolution profile information from the surface to 5 cm from NSP observations, and WCR observations below 5 cm. The Wang-Schmugge mixing scheme was used in the FR simulations ('FR/WS') based on mean 0-5 cm water content derived from NSP measurements. The 0-5 cm layer was chosen based on previous studies showing this to be the approximate emitting depth for L-band radiation [8, 21]. Simulations were performed for times when nearly coincident near-surface profile and SLMR observations were made. On most days from 17-26 June, these measurements were taken once, but on a few days multiple observations were made. This resulted in 10 model simulations for the Bare plot, 14 for Corn-2 and 11 for Corn-4.

B. Simulations with synthetic uniform profiles

Because the FR model determines brightness temperatures from mean near-surface moisture values and effective surface temperature, as opposed to the CRT which utilizes moisture and temperature profiles, we performed model simulations based on synthetic uniform profiles to eliminate model differences due to near-surface gradients and isolate variations due solely to the radiobrightness and mixing models. Uniform moisture profiles from 5% to 45% VWC in increments of 5% were generated, and the soil temperature was fixed at 300 K. Soil and vegetation properties for the Bare plot were used.

V. Results

A. Dielectric Constant

Model estimates of the real part of the soil dielectric constant, or permittivity, were compared with WCR permittivity estimates (adjusted for the previously-discussed WCR wet bias) for the Bare, Corn-2 and Corn-4 plots at 3 cm depth, the midpoint of the 1-5 cm layer sampled by the WCRs. For consistency with the FR/WS model, which is based on 0-5 cm mean conditions, mean 0-5 cm permittivity values from CRT/Dobson and CRT/WS were calculated as a weighted mean from individual model layers. From scatter plots of WCR- and model-estimated permittivity (not shown), two conclusions can be drawn. For all plots and times, the Dobson mixing scheme produced the highest permittivities; this is consistent with results shown in fig. 1. Also, the CRT/WS and FR/WS models produced essentially identical mean 0-5 cm permittivities. The very small differences are due to the fact that permittivity is calculated for each layer in CRT/WS, but a single value is calculated in FR/WS based on the mean 0-5 cm layer moisture and temperature. This indicates that using mean 0-5 cm soil moisture in the FR/WS model, as compared to using discrete profile values in the CRT/WS, does not have a significant impact on the near-surface dielectric constant and is simply a consequence of the nearly linear relationship between VWC and permittivity in the dielectric mixing schemes.

Statistics related to the comparison of model and WCR estimates are given for each plot in Table III. For bare soil, the CRT/Dobson model generally overestimates permittivity with respect to WCR-derived estimates, whereas the CRT/WS and FR/WS models underestimates permittivity by a similar amount. Correlations and root mean square differences (RMSD) are very similar between the models, and there is no clearly superior model. For Corn-2, the CRT/Dobson model again overestimates permittivity, while the CRT/WS and FR/WS model estimates agree very well with the observations, with small negative biases. Correlations among the models are nearly equal, and are the highest among the three

plots. RMSD values are much smaller for the CRT/WS and FR/WS than for CRT/Dobson. For Corn-4, CRT/Dobson permittivity estimates are virtually unbiased, whereas the CRT/WS and FR/WS models substantially underestimate permittivity. Correlations between the models are equal, and the CRT/Dobson model produces the lowest RMS differences.

B. Brightness Temperature – Uniform Soil Profiles

Variations in brightness temperatures between models may be attributed either to differences in estimates of dielectric constant or to the radiobrightness models' relationships between dielectric constant and T_B. Differences in dielectric constant resulting from the choice of mixing scheme were shown in fig. 1. Results from simulations using uniform moisture and temperature profiles are useful for illustrating model differences in the permittivity-brightness temperature relationship. In Fig. 2, we show brightness temperatures estimated by the CRT/Dobson, CRT/WS and FR/WS models, as a function of permittivity, for the bare soil uniform profiles. In theory, these differences should be negligible, as the CRT is equivalent to the Fresnel model for the case of uniform profiles. As expected, T_B differences are extremely small – less than 2 K except for very dry soil (small ε). For $\varepsilon < 5$, the CRT/Dobson and CRT/WS models estimate somewhat lower T_B than does the FR/WS model due to the approximation of the integral in (8) by a finite sum in the CRT model. The contributing depth of microwave radiation is believed to be greater for very dry soil than for wet soil [6, 17], and thus, there is some contribution to the emitted energy, albeit small, from the deep soil. In our simulations, the CRT model integrations were performed to 70 cm, and the slightly lower CRT-estimated brightness temperatures for $\varepsilon < 5$, relative to the FR/WS model, reflect the small errors resulting from the finite integration depth. For $\varepsilon > 5$, the differences of less than 1 K between CRT/WS and FR/WS are likely due to the inclusion of the imaginary part of the dielectric constant in the CRT.

A model comparison of brightness temperature as a function of soil moisture is presented in Fig. 3 for the bare soil uniform soil profiles. This represents the combined effect of the dielectric mixing schemes and the radiobrightness models in determining brightness temperature from VWC. Because radiobrightness model differences in the dielectric constant-T_B relationship are very small (fig. 2), the brightness temperature differences apparent in fig. 3 are due almost entirely to the two dielectric mixing scheme used (fig. 1). These departures are small at each end of the moisture scale and are greatest at intermediate moisture values, ranging between about 15 K at 10% to about 5 K at 30% VWC. Applied in an inverse mode to retrieve soil moisture, a 15 K difference in T_B would translate to approximately a 4% VWC difference for bare soil conditions.

C. Brightness Temperature – Observed Soil Profiles

Brightness temperatures estimated in model simulations using observed moisture and temperature profiles are compared with SLMR-measured T_B for the three plots in Figs. 4-6. Associated error statistics are given in Table IV. For all plots, the CRT/Dobson and FR/WS models underestimate observed brightness temperatures, whereas CRT/WS tends to overestimate T_B. None of the models stands out as producing better T_B estimates across all three plots. Correlations are slightly higher for FR/WS than for CRT/Dobson and CRT/WS. Based on RMS differences, the best results were obtained using the FR/WS model for the Bare plot, CRT/WS for Corn-2, and CRT/Dobson for Corn-4. The range of brightness temperature decreases dramatically with vegetation density from Bare to Corn-4. In terms of RMSD, model performance improves with the amount of vegetation. This is probably because of the lower range of T_B and the fact that the vegetation imparts a relatively constant signal that masks out

much of the day-to-day variability. On the other hand, correlations are quite high for the Bare and Corn-2 plots, but significantly lower for the CRT/Dobson and CRT/WS for Corn-4.

A comparison of results in Tables III and IV shows that, for the observed moisture and temperature profiles in Hsv98, the CRT model systematically estimates higher T_B than does the FR model, even when the same mixing scheme (WS) is used and the mean 0-5 cm permittivities are very similar. For example, at Corn-4, the CRT/WS model estimates a slightly higher mean permittivity than does the FR/WS model, implying a lower brightness temperature. However, the mean T_B estimated by CRT/WS is almost 10 K higher than the mean FR/WS-estimated T_B. Results are similar for the other two plots. A closer look at the Corn-4 moisture profiles (not shown) reveals the reason. For every observation used in the analysis, the uppermost (0-3 cm) soil layer is drier than the 0-5 cm layer, the latter of which is used to define the moisture content in the FR/WS model. The CRT model determines the emitted microwave energy using layers of 0.7 cm thickness and thus simulates the near-surface moisture gradients. Because brightness temperature is most sensitive to the uppermost soil conditions, the CRT/WS model estimates higher T_B than does the FR/WS model, which simulates a homogeneous 5 cm layer. The higher vertical resolution of the CRT results in a greater range of brightness temperature estimates compared to the Fresnel model because of the latter's simplistic treatment of the surface layer.

Because the correlations between modeled and measured brightness temperatures are very consistent and quite high, most of the difference in RMSD among the models is due to the systematic component, i.e. bias differences. Each model has its own aforementioned tendency toward higher or lower permittivity and consequent T_B. Because of uncertainties in soil and vegetation properties and in the empirical algorithms used to account for surface roughness and vegetation effects, in a particular set of simulations the resulting biases may either negate or augment one another. Therefore, any perceived

advantage of one model over the others for a certain set of conditions (soil, vegetation, etc.) may be misleading.

VI. Summary and Conclusions

This paper presents a comparison of two radiobrightness models, a multi-layer coherent radiative transfer model and a Fresnel reflectance-based single-layer model. Two soil dielectric mixing schemes are used along with the radiobrightness models to calculate the dielectric constant from observed and synthetic moisture and temperature profiles. Brightness temperature and permittivity estimated by the models are validated using measurements from the Huntsville '98 field experiment.

Some systematic model differences are observed. These can be attributed to (1) the mixing scheme, (2) the radiobrightness model itself, or (3) the representation of vertical profiles. Our numerical experiment was designed to quantify the sources of variation. Differences due to the mixing scheme were investigated through simulations in which uniform moisture and temperature profiles were used as model input. In these simulations, the Wang-Schmugge mixing scheme estimated lower permittivity and higher T_B than the Dobson mixing scheme. The difference can be as much as 15 K for soil moisture between 10% and 20% VWC. This T_B difference is equivalent to about a 4% difference in VWC. For uniform profiles, differences in T_B estimated by the two radiobrightness models, for a given dielectric constant, were very small (< 2 K). On the other hand, for cases using observed moisture and temperature profiles, the shape of the moisture profile (driest at the surface) in the coherent radiative transfer model resulted in T_B values 6-10 K higher than values estimated by the Fresnel model, which represents the soil as a uniform 5 cm slab.

No radiobrightness/mixing scheme combination exhibited superiority across all plots and times (i.e. different conditions). There are small to moderate model-to-model differences in dielectric constant and brightness temperature. Each model agrees quite well with dielectric constant and brightness temperature measurements. There is some degree of uncertainty in model parameters and variables related to soil and vegetation properties, as well as in the measurements used as model input and validation. In some cases, these errors may offset model biases, while at other times the errors may be additive. Therefore, it is difficult to conclude with confidence which model is superior. However, the results imply that a multiple layer radiative transfer model is more effective than a single-layer model in situations where the near-surface moisture or temperature gradients are, provided that reasonably accurate information about the gradients is available.

VII. Acknowledgements

We acknowledge F. Archer, J. Boggs, T. Coleman, A. Fahsi, S. Hostler, A. Manu, J. Martinez, G. Robertson, Z. Senwo, W. Tadesse, T. Tsegaye and Alabama A&M University's Center for Hydrology, Soil Climatology and Remote Sensing (HSCaRS) support staff for invaluable assistance during the field experiment. We appreciate our useful discussions with Eni Njoku regarding the CRT model. We also acknowledge Jim Bilskie from Campbell Scientific, Inc. for useful discussions regarding the Water Content Reflectometers. Any use of trade, product or firm names is for descriptive purposes only and does not imply endorsement by the U.S. Government.

VIII. References

[1] T. J. Jackson, T. J. Schmugge, R. Parry, W. P. Kustas, J. C. Ritchie, A. M. Shutko, A. Haldin, E. Reutov, E. Novichikhin, B. Liberman, J. C. Shiue, M. R. Davis, D. C. Goodrich, S. B. Amer, and L. B. Bach, "Multifrequency passive microwave observations of soil moisture in an arid rangeland environment," *Int. J. Rem. Sens.,* vol. 13**,** pp. 573-580, February 1992.

[2] T. J. Jackson, D. M. LeVine, A. J. Griffis, D. C Goodrich, T. J. Schmugge, C. T. Swift, and P. E. O'Neill, "Soil moisture and rainfall estimation over a semiarid environment with the ESTAR microwave radiometer," *IEEE Trans. Geosci. Remote Sensing.,* vol. 31, pp. 836-841, July 1993.

[3] V. Lakshmi, E. F. Wood, and B. J. Choudhury, "Evaluation of Special Sensor Microwave/Imager satellite data for regional soil moisture estimation over the Red River Basin," *J. Appl. Meteor.,* vol. 36**,** pp. 1309-1328, October 1997.

[4] Y.-A. Liou, J.F. Galantowicz and A.W. England, "A land surface process/radiobrightness model with coupled heat and moisture transport for prairie grassland," *IEEE Trans. Geosci. Remote Sensing,* vol. 31, pp. 1848-1859, July 1999.

[5] S. Raju, A. Chanzy, J.-P. Wigneron, J.-C. Calvet, Y. Kerr and L. Laguerre, "Soil moisture and temperature profile effects on microwave emission at low frequencies," *Rem. Sens. Environ.,* vol. 54, pp. 85-97, November 1995.

[6] E. T. Engman and N. Chauhan, "Status of microwave soil moisture measurements with remote sensing," *Rem. Sens. Environ.*, vol. 51, pp. 189-198, January 1995.

[7] T. J. Jackson, P. E. O'Neill, and C. T. Swift, "Passive microwave observation of diurnal surface soil moisture," *IEEE Trans. Geosci. Remote Sensing*, vol. 35, pp. 1210-1222, September 1997.

[8] T. J. Jackson, "Measuring surface soil moisture using passive microwave remote sensing," *Hyd. Proc*., vol. 7, pp. 139-152, January 1993.

[9] D. Entekhabi, H. Nakamura, and E. G. Njoku, "Solving the inverse problem for soil moisture and temperature profiles by sequential assimilation of multifrequency remotely sensed observations," *IEEE Trans. Geosci. Rem. Sensing,* vol. 32, pp. 438-448, March 1994.

[10] J.F. Galantowicz, D. Entekhabi and E.G. Njoku, "Tests of sequential data assimilation for retrieving profile soil moisture and temperature from observed L-Band radiobrightness," *IEEE Trans. Geosci. Remote Sensing*, vol. 37, pp. 1860-1870, July 1999.

[11] E.G. Njoku and L. Li, "Retrieval of land surface parameters using passive microwave measurements at 6-18 GHz," *IEEE Trans. Geosci. Remote Sensing*, vol. 37, pp. 79-93, January 1999.

[12] T. Schmugge and B.J. Choudhury, "A comparison of radiative transfer models for predicting the microwave emission from soils," *Radio Science,* vol. 16, pp. 927-938, September-October 1981.

[13] E. G. Njoku and N.-A. Kong, "Theory for passive microwave remote sensing of near-surface soil moisture," *J. Geophys. Res.,* vol. 82**,** pp. 3108-3118, July 1977.

[14] E.G. Njoku and P.E. O'Neill, "Multifrequency microwave radiometer measurements of soil moisture," *IEEE Trans. Geosci. Remote Sensing*, vol. 20, pp. 468-475, October 1982.

[15] J. R. Wang and T. J. Schmugge, "An empirical model for the complex dielectric permittivity of soils as a function of water content," *IEEE Trans. Geosci. Remote Sensing,* vol. 18, pp. 288-295, October 1980.

[16] M. C. Dobson, F. T. Ulaby, M. T. Hallikainen, and M. A. El-Rayes, "Microwave dielectric behavior of wet soil-Part II: Dielectric mixing models," *IEEE Trans. Geosci. Remote Sensing*, vol. 23**,** pp. 35-46, January 1985.

[17] F. T. Ulaby, R. K. Moore and A. K. Fung, "*Microwave Remote Sensing, Active and Passive, vol.III: From Theory to Applications*," Boston, MA: Artech House, 1986.

[18] B. J. Choudhury, T. J. Schmugge, A. Chang, and R. W. Newton, "Effect of surface roughness on the microwave emission from soils," *J. Geophys. Res.,* vol. 84, pp. 5699-5706, September 1979.

[19] T. J. Jackson, and T. J. Schmugge, "Vegetation effects on the microwave emission of soils," *Rem. Sens. Environ.*, vol. 36, pp. 203-212, June 1991.

[20] L. A. Klein and C. T. Swift, "An improved model for the dielectric constant of sea water at microwave frequencies," *IEEE Trans. Antennas and Propagation*, vol. 25, pp. 104-111, January 1977.

[21] T. J. Jackson and T. J. Schmugge, "Passive microwave remote sensing system for soil moisture: Some supporting research," *IEEE Trans. Geosci. Remote Sensing*, vol. 27**,** pp. 225-235, March 1989.

[22] F. Baret, G. Guyot and D. J. Major, "Crop biomass evaluation using radiometric measurements," *Photogrammetrica*, vol. 43, pp. 241-256, 1989.

[23] J. P. Wigneron, A. Chanzy, J. C. Calvert and N. Bruguier, "A simple algorithm to retrieve soil moisture and vegetation biomass using passive microwave measurements over crop fields," *Remote Sens. Environ*., vol. 51, pp. 331-341, March 1995.

[24] M. A. Gilabert, S. Gandia and J. Melia, "Analyses of spectral-biophysical relationships for a corn canopy," *Remote Sens. Environ*., vol. 55, pp. 11-20, January 1996.

[25] C. A. Laymon, W.L. Crosson, T.J. Jackson, A. Manu, V. Soman and T.D. Tsegaye, " Ground-based passive microwave remote sensing observations of soil moisture at S and L band with insight into measurement accuracy", *IEEE Trans. on Geosci. and Rem. Sens*., in press.

[26] B. J. Choudhury, T. J. Schmugge and T. Mo, "A parameterization of effective soil temperature for microwave emission," *J. Geophys. Res.*, vol. 87, pp. 1301-1304, February 1982.

Figure Captions

Fig. 1. Comparison of permittivity estimated by the Dobson and Wang-Schmugge mixing schemes as a function of volumetric water content.

Fig. 2. Brightness temperature as a function of permittivity estimated by all models for uniform profiles.

Fig. 3. Brightness temperature as a function of volumetric water content estimated by all models for uniform profiles.

Fig. 4. Comparison of brightness temperature from all models with SLMR measurements for 10 observation times for the Bare plot.

Fig. 5. Comparison of brightness temperature from all models with SLMR measurements for 14 observation times for the Corn-2 plot.

Fig. 6. Comparison of brightness temperature from all models with SLMR measurements for 11 observation times for the Corn-4 plot.

Table Captions

Table I. Percent errors and range of permittivity estimates obtained from Water Content Reflectometer measurements.

Table II. Definitions, values and data sources for model variables.

Table III. Statistics related to model and measured permittivities.

Table IV. Statistics related to model and measured brightness temperatures.

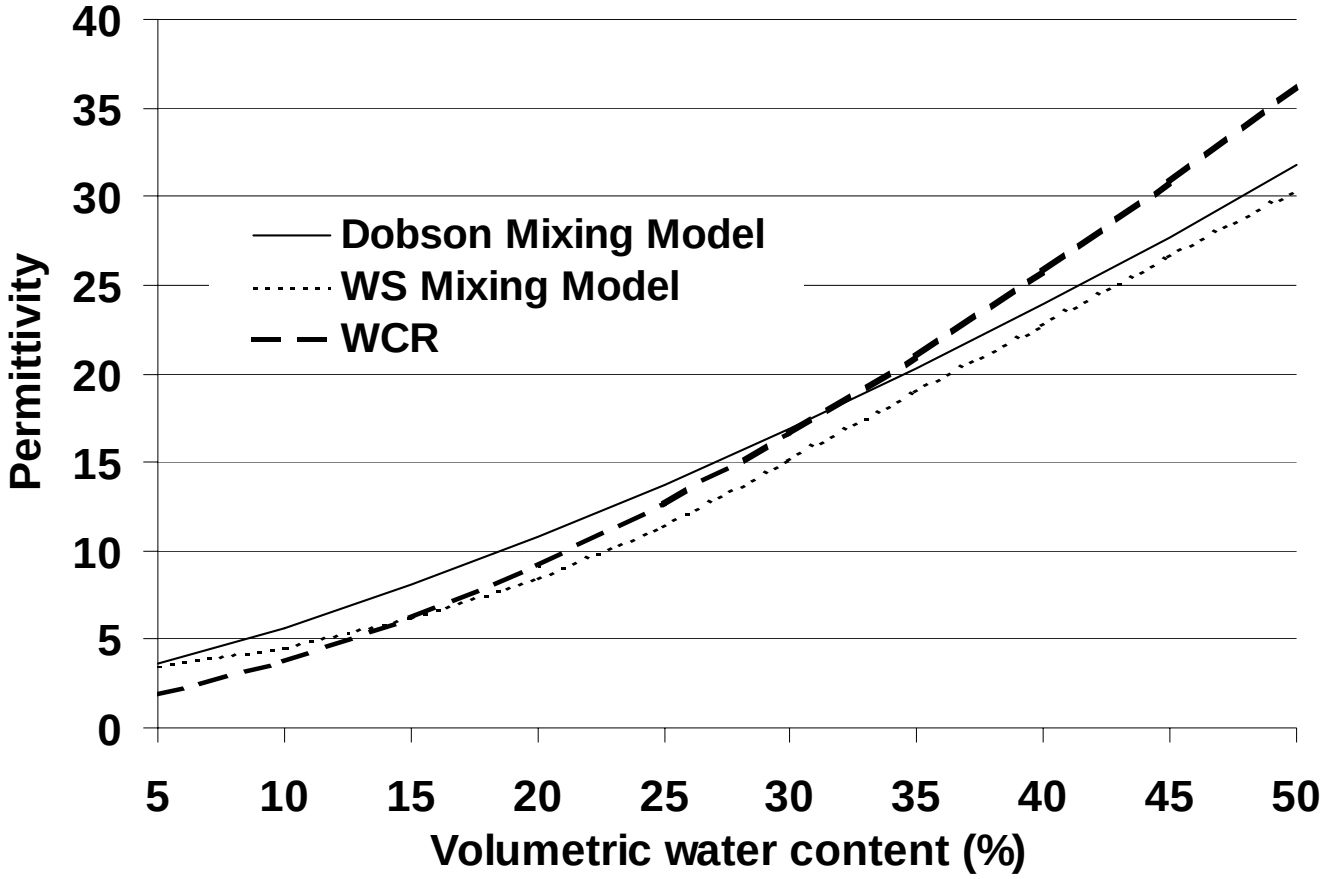
40
35
30
25
20
15
10
5
0
Permittivity
Dobson Mixing Model
WS Mixing Model
WCR
5
10
15
20
25
30
35
40
45
50
Volumetric water content (%)

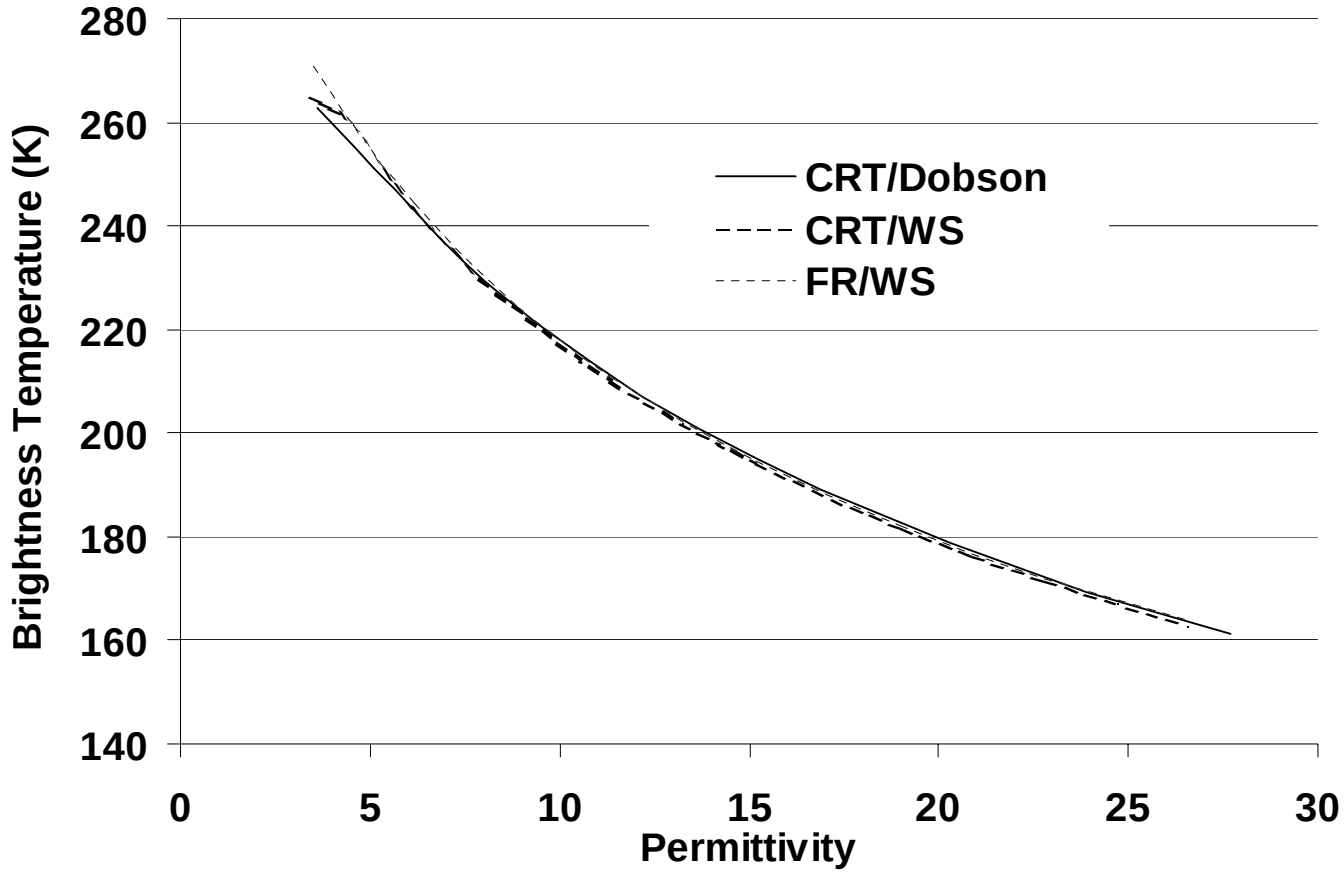
280
260
240
220
200
180
160
140
Brightness Temperature (K)
0
5
10
15
20
25
30
Permittivity
CRT/Dobson
CRT/WS
FR/WS

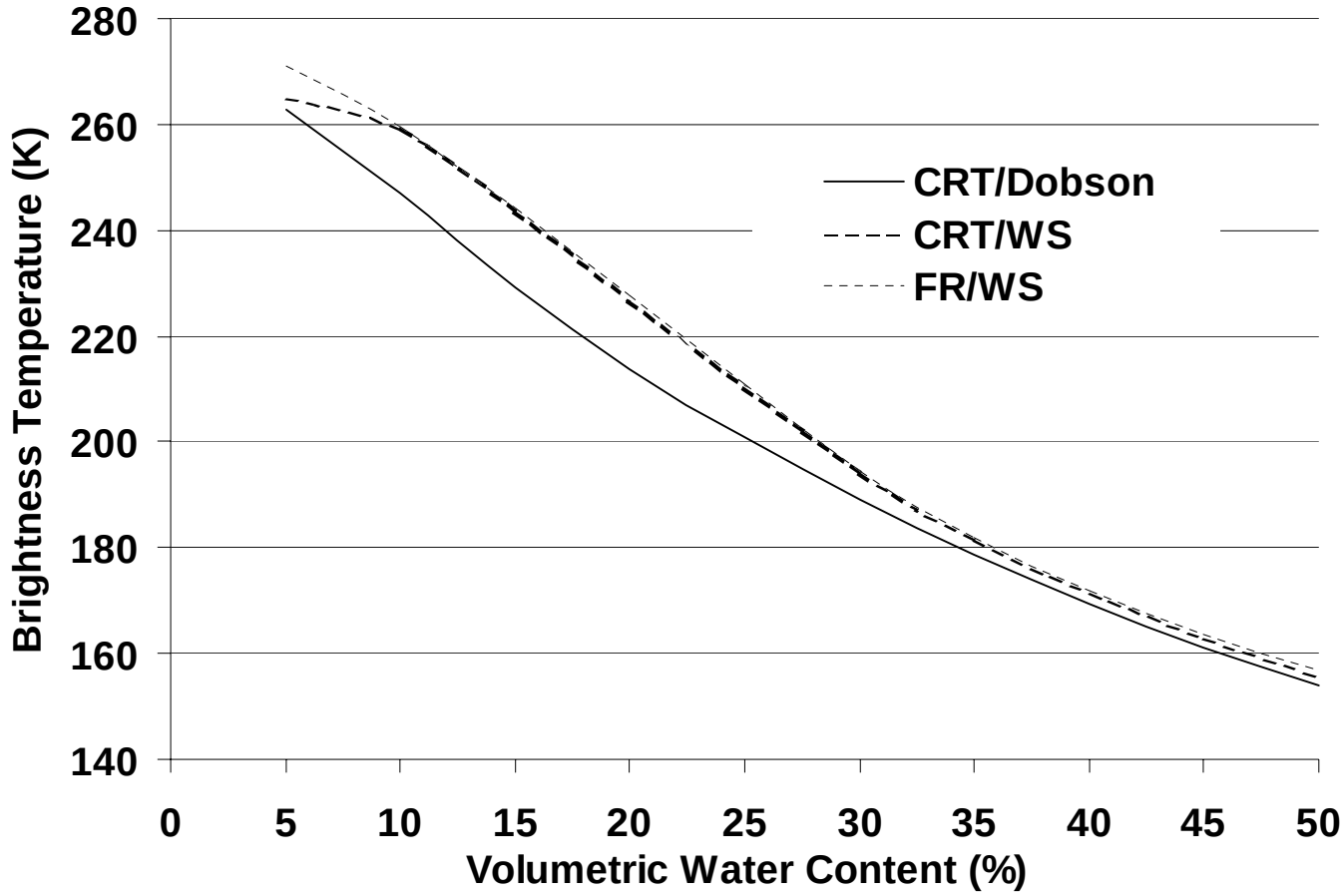
280
260
240
220
200
180
160
140
Brightness Temperature (K)
0
5
10
15
20
25
30
35
40
45
50
Volumetric Water Content (%)
CRT/Dobson
CRT/WS
FR/WS

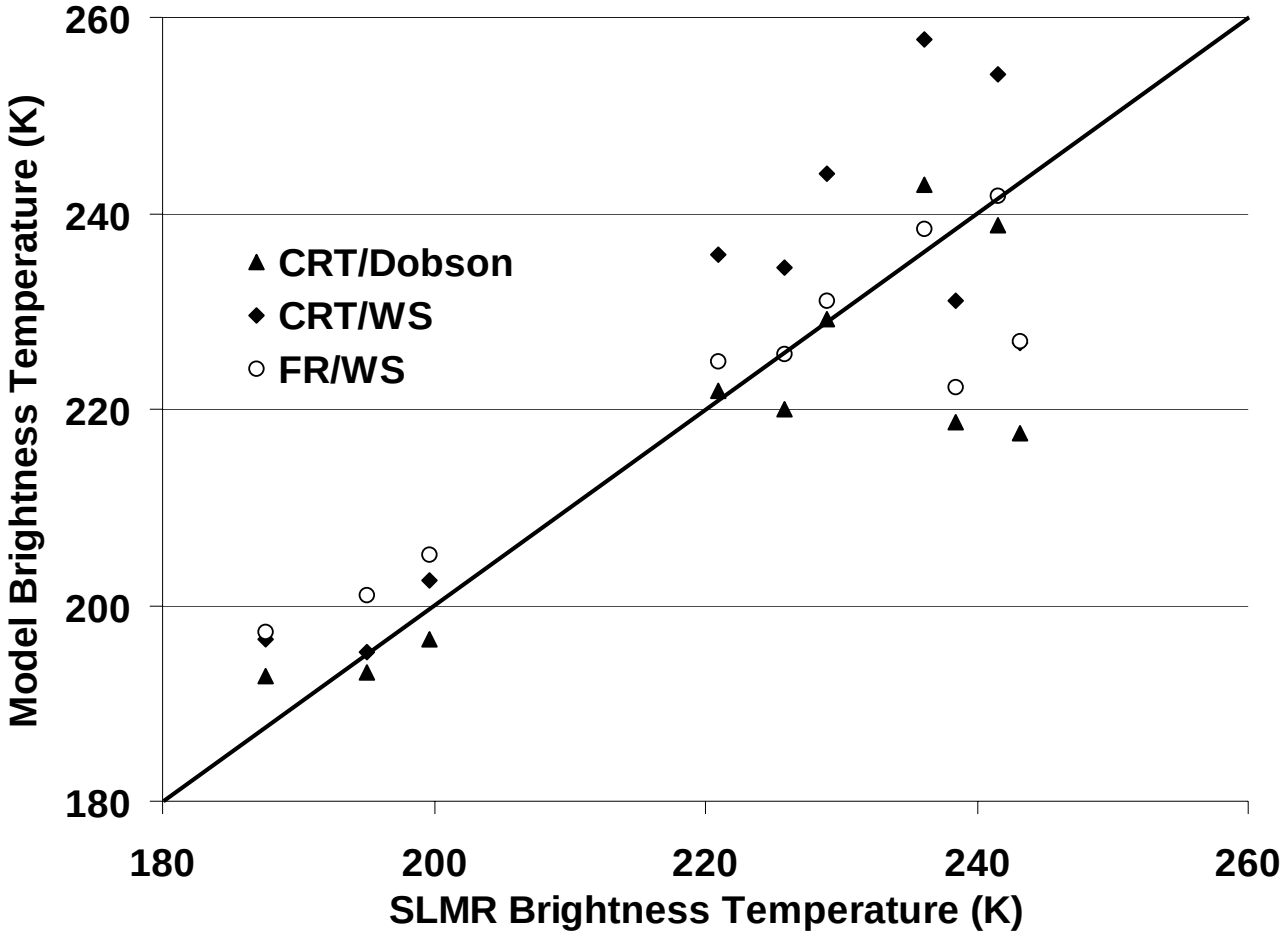
260
240
220
200
180
Model Brightness Temperature (K)
CRT/Dobson
CRT/WS
FR/WS
180
200
220
240
260
SLMR Brightness Temperature (K)

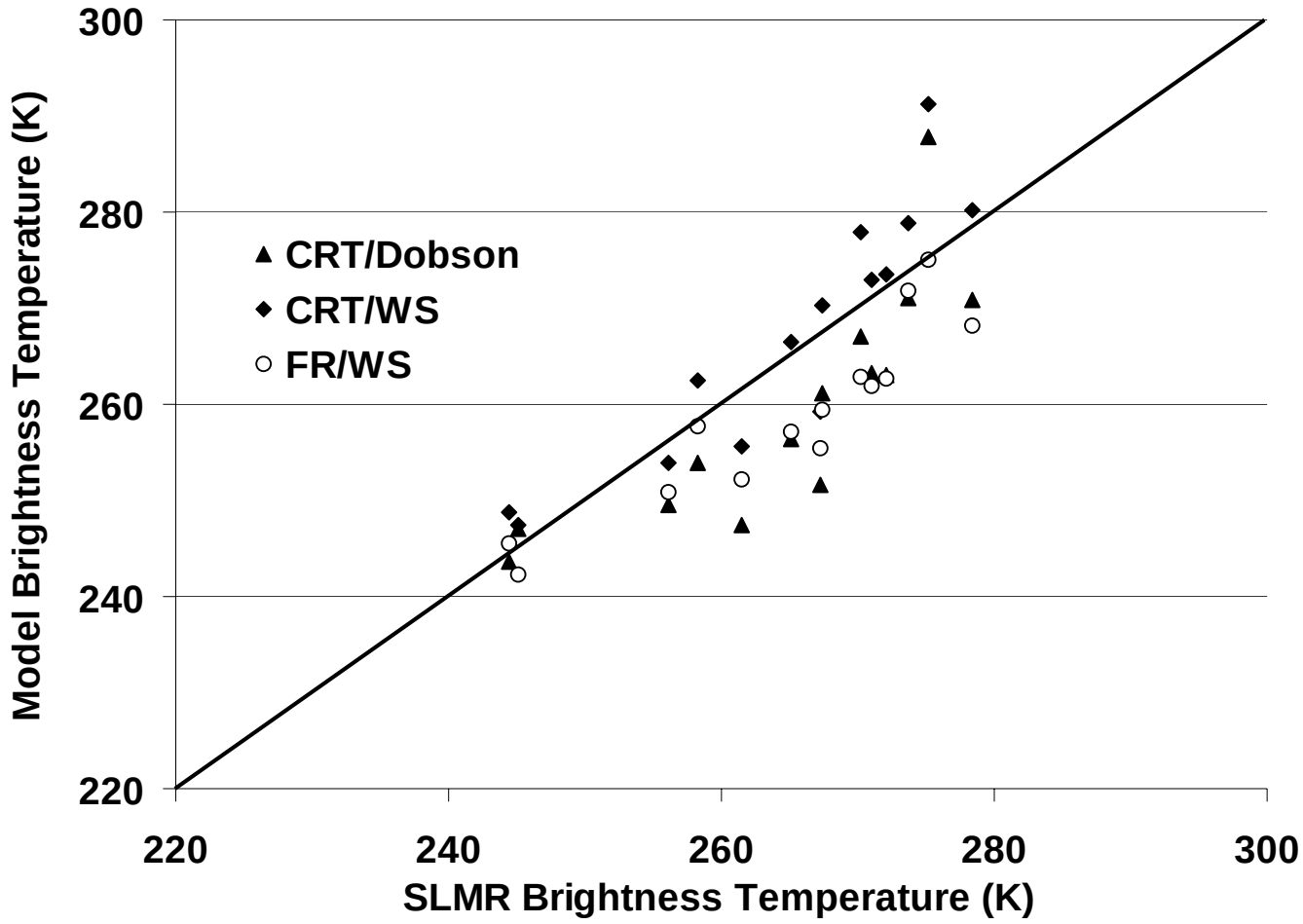
300
280
260
240
220
Model Brightness Temperature (K)
CRT/Dobson
CRT/WS
FR/WS
220
240
260
280
300
SLMR Brightness Temperature (K)

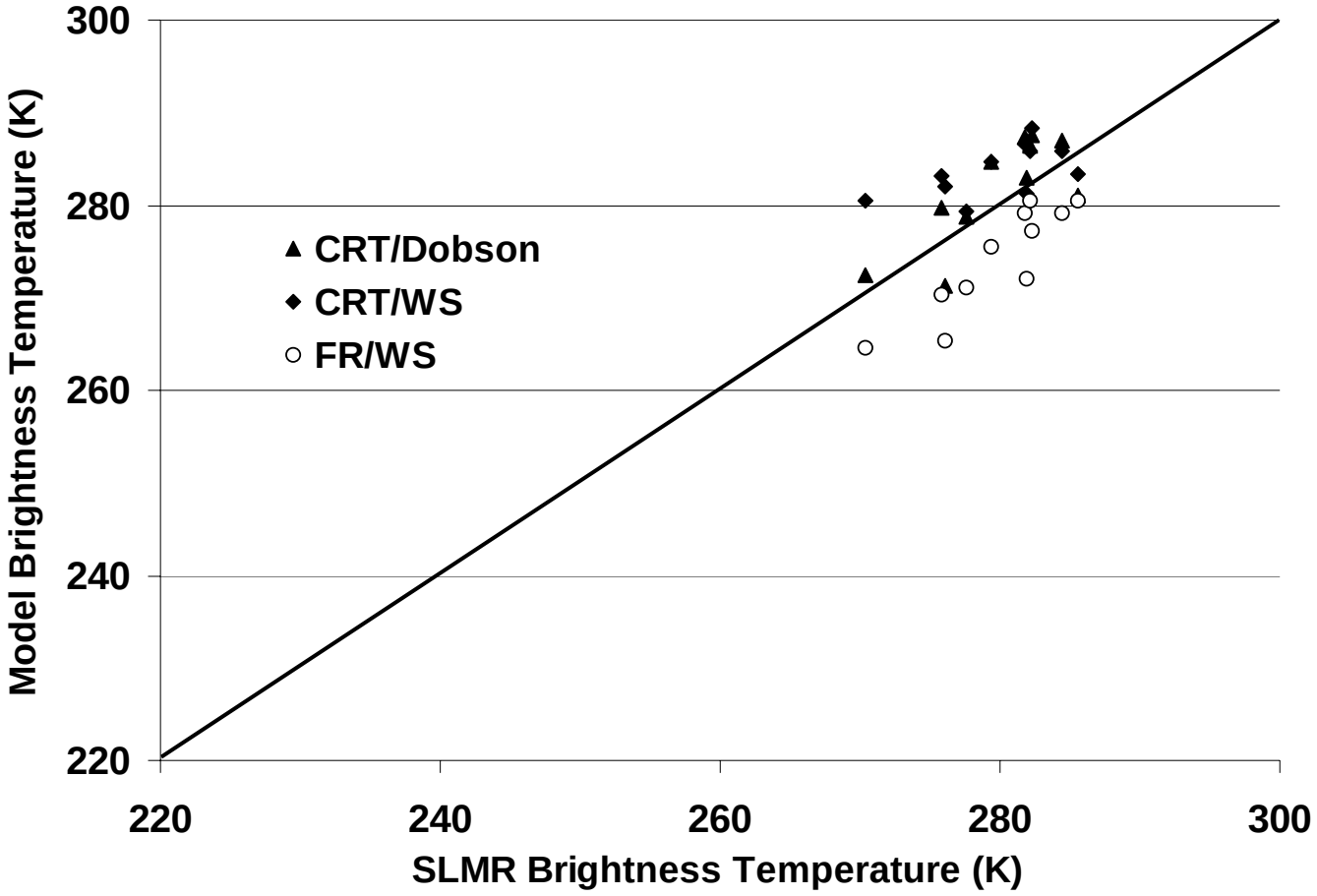
300
280
260
240
220
Model Brightness Temperature (K)
CRT/Dobson
CRT/WS
FR/WS
220
240
260
280
300
SLMR Brightness Temperature (K)

TABLE I

PERCENT ERRORS AND RANGE OF PERMITTIVITY ESTIMATES OBTAINED FROM WATER CONTENT REFLECTOMETER MEASUREMENTS.

Permittivity (ε)	**% error in ε**	**Minimum**	**Maximum**
5 (very dry)	10.3	4.5	5.5
10 (moderately dry)	7.2	9.3	10.7
15 (moist)	5.9	14.2	15.9
20 (wet)	5.1	19.0	21.0

TABLE II
DEFINITIONS, VALUES AND DATA SOURCES FOR MODEL VARIABLES.

Variable definition	Units	Bare	Corn-2	Corn-4	Data source
SLMR Variables					
Microwave frequency	GHz	1.413	1.413	1.413	SLMR configuration
Radiometer look angle	degrees	15	15	15	SLMR configuration
Soil Variables					
Sand content	%	15	10	10	Field measurements
Clay content	%	20	25	25	Field measurements
Bound water content in soil	$m^3 \bullet m^{-3}$	0.04	0.05	0.05	[16, 21]
Surface RMS roughness	cm	0.3	0.1	0.1	Estimated from field measurements
Soil porosity (Variation w/depth in CRT)	unitless	0.53 (0.40-0.57)	0.51 (0.40-0.61)	0.51 (0.36-0.59)	Field measurements
Deep soil (10 m) temperature (CRT)	Kelvins	291	291	291	Annual mean temperature
Empirical coefficient in Dobson mixing model	unitless	0.65	0.65	0.65	[16]
Vegetation Variables					
Vegetation water content	$kg \bullet m^{-2}$	0.0	1.9-2.5	3.2-4.5	Field measurements
B-parameter in vegetation correction	$m^2 \bullet kg^{-1}$	N/A	0.11	0.11	[19]

TABLE III
STATISTICS RELATED TO MODEL AND MEASURED PERMITTIVITIES FOR THE 0-5 CM SOIL LAYER.

Bare Plot Adjusted 3 cm WCR permittivity = 11.03	**CRT/Dobson**	**CRT/WS**	**FR/WS**
Mean	12.13	9.96	9.87
Mean Bias	1.10	-1.07	-1.16
Correlation	0.91	0.91	0.91
RMS Difference	1.44	1.46	1.56
Corn-2 Plot Adjusted 3 cm WCR permittivity = 8.46			
Mean	10.34	8.11	7.74
Mean Bias	1.87	-0.35	-0.73
Correlation	0.92	0.93	0.94
RMS Difference	2.06	0.80	0.99
Corn-4 Plot Adjusted 3 cm WCR permittivity = 8.95			
Mean	8.83	6.79	6.64
Mean Bias	-0.11	-2.16	-2.30
Correlation	0.79	0.79	0.79
RMS Difference	1.81	2.92	3.03

TABLE IV
STATISTICS RELATED TO MODEL AND MEASURED BRIGHTNESS TEMPERATURES.

Bare Plot SLMR Brightness Temperature = 221.7	**CRT/Dobson**	**CRT/WS**	**FR/WS**
Mean (Kelvins)	217.2	227.8	221.4
Mean Bias (Kelvins)	-4.6	6.1	-0.3
Correlation	0.86	0.86	0.92
RMS Difference (Kelvins)	10.9	12.5	8.4
Corn-2 Plot SLMR Brightness Temperature = 264.7			
Mean (Kelvins)	259.6	267.1	258.8
Mean Bias (Kelvins)	-5.1	2.4	-5.9
Correlation	0.82	0.90	0.91
RMS Difference (Kelvins)	8.8	4.7	7.8
Corn-4 Plot SLMR Brightness Temperature = 279.8			
Mean (Kelvins)	281.8	283.7	274.1
Mean Bias (Kelvins)	2.0	4.0	-5.6
Correlation	0.78	0.58	0.89
RMS Difference (Kelvins)	3.9	5.2	5.5